Controlling the Structure of a Porous Polymer by Coupling Supercritical CO_2 and Single Screw Extrusion Process

Clémence Nikitine,[1,2] Elisabeth Rodier,[1,3] Martial Sauceau,[1,3] Jean-Jacques Letourneau,[1,3] Jacques Fages[1,3]

[1]*Ecole des Mines d'Albi, RAPSODEE research centre, Albi F-81013, France*
[2]*Université de Lyon, CPE-LGPC, UMR 2214, Villeurbanne F-69100, France*
[3]*Université de Toulouse, Mines Albi, CNRS, Albi F-81013, France*

Received 8 January 2009; accepted 23 June 2009
DOI 10.1002/app.31031
Published online 15 September 2009 in Wiley InterScience (www.interscience.wiley.com).

ABSTRACT: A study on the extrusion of Eudragit E100 was carried out using supercritical carbon dioxide ($scCO_2$) as plasticizer and foaming agent. $ScCO_2$ modifies the rheological properties of the material in the barrel of the extruder and acts as a blowing agent during the relaxation when flowing through the die. For experiments, a single-screw extruder was modified to be able to inject $scCO_2$ within the extruded material. The aim is to determine a correlation between operating conditions and foam structure. The effect of three parameters was studied: the temperature in the die and in the metering zone, the screw speed, and the volumetric flow rate of CO_2. An increase in temperature enhances the expansion rate and the average pore diameter and appears to be the most significant parameter. The effect of CO_2 concentration is significant at small concentrations only: the higher the CO_2 concentration, the lower the pore density and the higher both the pore diameter and the expansion rate. The effect of the screw speed is tricky because a variation of this speed involves a decrease of CO_2 weight ratio. This study shows that the structure of the extrudates does not evolve with a coupling of screw speed increase and a subsequent CO_2 weight ratio decrease. © 2009 Wiley Periodicals, Inc. J Appl Polym Sci 115: 981–990, 2010

Key words: extrusion; polymer; supercritical carbon dioxide; Eudragit E100; foams

INTRODUCTION

Although many different materials can be extruded, which means forced through a die, polymers are nowadays the main industrial application of such process. Among the three categories of polymers, thermoplastics, thermosets, and elastomers, the thermoplastics are, by far, the most processed by extrusion since their chemical nature and structure remained unchanged by undergoing extrusion.[1]

Manufacturing polymeric foams has more recently drawn researchers interest due to their multiple applications in acoustic dampening, thermal insulation, microelectronic applications as well as controlled release pharmaceutical formulations and scaffolds for living tissue in biomedicine. Conventional foams are produced using either chemical or physical blowing agents. Various chemical blowing agents, which are generally low molecular weight organic compounds, are mixed with a polymer matrix and decompose when heated beyond a threshold temperature. This results in the release of a gas, and thus, the nucleation of bubbles. This implies, however, the presence of residues in the porous material and the need for an additional stage to eliminate them.

An alternative lies in the use of a supercritical fluid (SCF). SCFs allow fast mass transfers due to their gas-like diffusivity, liquid-like density, low viscosity, and surface tension.[2] In particular, supercritical carbon dioxide ($scCO_2$), which is considered as a green solvent in spite of its effect on the global warming, has emerged as an important SCF. In addition to its non-toxicity, non-flammability, and chemical inertia, it displays accessible supercritical conditions (Tc = 31.1°C, Pc = 7.38 MPa). In the supercritical domain, it is relatively easy to fine tune its physicochemical properties from vapor-like to liquid-like limits by varying pressure and/or temperature. $ScCO_2$ is also known for being soluble in large proportions in many polymers and has already been used in polymer processing.[3–6] Dissolved $scCO_2$ acts as a plasticizer leading to changes in mechanical and physical properties which in turn would decrease the constraints undergone by the material. The glass transition temperature, the interfacial tension, or the viscosity of various polymers could be lowered by $scCO_2$, without changing the viscoelastic behavior of the polymer matrix.[7]

Presence of $scCO_2$ in extrusion process modifies rheological properties of the polymer in the barrel of

Correspondence to: C. Nikitine (clemence.nikitine@cpe.fr).

the extruder and acts as a blowing agent during the relaxation when flowing through the die.[8] Thus, its relatively high solubilisation in the polymer results in extensive expansion at the die. The reduction of viscosity decreases the mechanical constraints and the operating temperature within the extruder. Thus, coupling extrusion and $scCO_2$ would allow the use of fragile or thermolabile molecules, like pharmaceutical molecules. The absence of residues in the final material is also an advantage for a pharmaceutical application.

In classical theory, the homogeneous nucleation rate (i.e., the number of cells created per unit of time and volume) can be expressed as a function of the Gibbs free energy barrier for the formation of a critical bubble nucleus and temperature.[9] The theory suggests that the surface tension diminution or the saturation pressure increase will result in the increase of nucleation rate and the number of bubbles created. Moreover, the power 3 of the surface tension in the expression of the free energy will involve a higher influence on nucleation. The interfacial tension decreasing with the pressure,[10] $scCO_2$ allows thus the bubbles to appear at lower energy threshold. Consequently, the homogeneous nucleation rate increases and a large number of small cells is obtained. In fact, controlling supercritical CO_2 quantity allows the modification of the cell density and the cell size in microcellular foaming.

Our lab has developed a supercritical carbon dioxide-assisted extrusion process, which has been applied to the polymer Eudragit E100. This polymer was chosen because of its pharmaceutical application and high enough CO_2 solubility to generate a substantial porosity (this was observed visually for a preliminary choice of the polymer). Moreover, Eudragit E100 has been already implemented by extrusion to produce solid dispersions of itraconazole[11,12] and also to design porous extrudates with injection of $scCO_2$.[13]

In a first stage, the residence time distribution (RTD) of a dye with and without the injection of $scCO_2$ was studied.[14] In this study, the aim is to observe the effects on the structure of polymeric foams of three operating parameters: the temperature in the metering zone and in the die, the screw speed and the mass flow rate of CO_2. This study has been performed to understand the different phenomena implied in extrusion process and to determine correlations between the operating conditions and the expansion, the cell size, and the cell density in macro or microcellular foaming. Some tests of compressive strength have also been carried out, but the extrudates were very fragile and they were crushed instantaneously. However, this research is not aimed at making scaffolds but rather matrices for solid dispersions of active molecules.

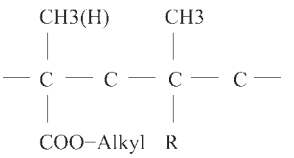

Figure 1 Monomer of Eudragit.

MATERIALS AND METHODS

Extrusion process

Eudragit E100 (SPCI, France) was used in different experiments. Eudragit polymers are copolymers derived of acrylic acid and methacrylate. Because of their multifunctional nature, unique properties, and good biocompatibility, these polymers are considered to be of pharmaceutical grade.[15]

Figure 1 shows a monomer of Eudragit polymer. In Eudragit E, the –alkyl group is an ethyl group (C_2H_6) and the –R group a aminoethyl/methacrylate ($-COOCH_2CH_2N(CH_3)_2$). Eudragit E are soluble in digestive fluids and are currently used as coating in solid pharmaceutical dosage forms for taste masking and protection.[16]

It is an amorphous polymer. Its glass transition temperature, measured by DSC (Differential Scanning Calorimetry, ATG DSC 111, SETARAM), is around 45–52°C. The solid density ρ_E, determined by helium pycnometry (Micromeretics, AccuPYC 1330) is 1104 kg/m^3. A rheological study at atmospheric pressure has been performed (ARES, Rheometric Scientific). The polymer viscosity decreases when shear rate increases, which is a characteristic behavior of a pseudoplastic fluid.[17] In addition, the viscosity is similar to those of molten polymers ($\cong 10^3$ Pa s). This characterization step helped in choosing the operating conditions to process Eudragit E100 by extrusion. These conditions have to ensure that the polymer flows well enough through the barrel without being thermally degraded and that CO_2 is dissolved enough in the polymer to create porosity.

Figure 2 shows the experimental set up (Escamex, France). The single-screw extruder used in this study has a 30 mm-screw diameter and a length to diameter ratio (L/D) of 35, that is to say a 1.05 m length (Rheoscam, SCAMEX). The screw is divided into three parts. The first one has a length to diameter ratio of 20 and the two others have a length to diameter ratio of 7.5. Between each part, a restriction ring has been fitted out to obtain a dynamic gastight (it prevents $scCO_2$ from backflowing). The first part has conical geometry to allow the transport of solid polymers and then, their melting and their plasticizing. Finally, the screw has a cylindrical geometry from the first gastight ring to the die. The temperature inside the barrel is regulated at five locations: T_a and

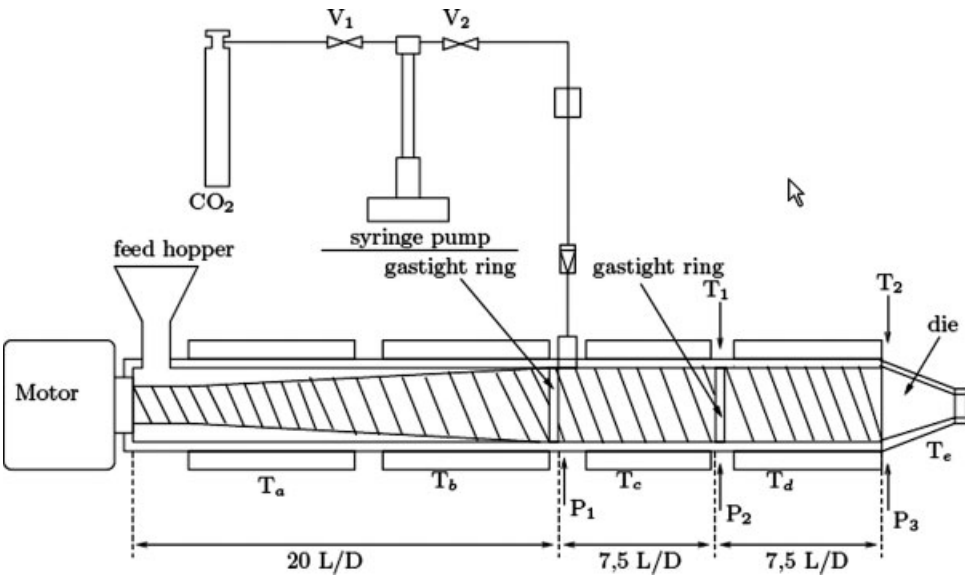

Figure 2 Experimental system.

T_b before the CO_2 injection, T_c and T_d after the injection, and T_e in the die. Only the temperature of the metering zone T_d and T_e were changed at each experiment. Four other temperatures were kept constant at 130°C.

Eudragit E100 is introduced into the feed hopper, and then flows through the barrel, begins to melt in the first part, is pressurized in the last two parts and is then forced through the die. There are three pressure sensors and two temperature sensors: P_1 after the CO_2 injector, P_2 and T_1 before the second gastight ring and P_3 and T_2 by the die. This allows measuring the temperature and the pressure of the polymer inside the extruder. Errors associated to pressure and temperature sensors were about 0.2 MPa and 3.3°C, respectively.

Carbon dioxide (N45, Air liquide) is pumped from a cylinder by a syringe pump (260D, ISCO), which allows small flow rates (i.e., 1 mm^3/s). The pump runs in a constant volumetric flow rate mode and CO_2 was introduced at the same pressure as the one inside the extruder. The CO_2 injector is positioned at a length to diameter ratio of 20 from the feed hopper. It corresponds to the beginning of the metering zone, that is to say the part where the channel depth is constant and equal to 1.5 mm. The pressure, the temperature, and the volumetric CO_2 flow rate are measured within the syringe pump. CO_2 density, obtained by Peng Robinson equation of state,[18] is used to calculate mass flow rate.

Experiments and structure analysis

For each experiment, carbon dioxide was then introduced at constant volumetric flow rate. The pressure in the CO_2 pump is kept slightly higher than the pressure P_1, measured at the injection point within the barrel. Once steady state conditions are reached, extrudates were collected and water-cooled to freeze the extrudate structure. Cooling was done at ambient temperature. About 10 samples were collected during the experiment to check the homogeneity of the extrudates.

The operating conditions, easily tuneable and suspected to be the most influent on the extrudates structure, are the die temperature T_e and the metering zone temperature T_d (during all the experiments, $T_d = T_e$ and will be referred as die temperature), the screw speed and the CO_2 volumetric flow rate. The temperatures in the zones of feeding and melting (corresponding to T_a, T_b, and T_c) were fixed at 130°C. Table I shows the operating parameters for each experiment. Extrusion tests were performed at die temperature ranging from 110 to 130°C on the basis of the rheological studies, to have molten polymer. The range of the screw speed was fixed by the constructor's parameters. Finally, it was necessary to have a permanent flow rate of polymer in the die; the maximum of the CO_2 flow rate was determined by the steady flow. Higher CO_2 content than studied range usually causes unstable polymer flow with oscillating pressure. The 15 first experiments correspond to an experimental design and the following ones were carried out to complete the data.

Cylinders of Eudragit E100, 0.8–1.2 mm of diameter, were obtained. To calculate the apparent porosity ρ_{app}, they were weighed (METTLER TOLEDO, AT400) and their volumes were evaluated by measuring their diameter and length with a vernier (Facom). To obtain this apparent density with a good enough precision, an average of 10 measurements was carried out. Expansion rate, defined as

TABLE I
Operating Conditions of the Experiments

No.	T (°C)	N (rpm)	Q_{CO_2} (cm^3/min)	C_{CO_2} (%)
1	110	40	0.05	0.126
2	130	40	0.05	0.089
3	110	80	0.05	0.068
4	130	80	0.05	0.046
5	110	40	0.15	0.381
6	130	40	0.15	0.271
7	110	80	0.15	0.202
8	130	80	0.15	0.137
9	120	60	0.1	0.164
10	120	60	0.1	0.164
11	120	60	0.1	0.164
12	130	40	0.05	0.089
13	110	80	0.15	0.202
14	125	50	0.07	0.105
15	115	70	0.12	0.128
16	130	40	0.001	0.002
17	130	40	0.01	0.018
18	110	40	0.001	0.002
19	110	40	0.01	0.025
20	110	40	0.1	0.254
21	130	20	0	0
22	130	40	0	0
23	130	40	0	0
24	130	60	0	0
25	130	80	0	0
26	140	40	0	0
27	150	40	0	0
28	130	40	0.1	0.178
29	130	40	0.1	0.178
30	130	40	0.05	0.092

the ratio of the extrudate volume (after extrusion) to the Eudragit E100 volume (before extrusion) is calculated by eq. (1).

$$\varepsilon = \frac{\rho_E}{\rho_{app}} \tag{1}$$

ρ_E is the Eudragit E100 density and ρ_{app} the apparent density of the extrudate.

To complete the characterization of the porosity structure, samples were examined by environmental scanning electron microscopy (ESEM, FEG, Philips). An image analysis software using the Image Processing Toolbox™ of Matlab®, has been designed in the laboratory to estimate the cell size and the cell density. This image processing task is mainly a watershed segmentation and can be declined in three main steps: first the enhancement of the image contrast and an exaggeration of the gaps between the pores are obtained by adding the "top-hat" filtered image and subtracting the "bottom-hat" filtered image to the original ESEM image. Then, the core of each pore is detected by computing the extended-minima transform[19] of the image that corresponds to a particular thresholded image of connected pixels less than a specific intensity value. Finally, a "watershed segmentation"[20] is accomplished using both the thresholded binary image and the enhanced one. The labeled regions so obtained give a good representation of the pore distribution in a section of an Eudragit extrudate. For each section, the number of pores, their area, average diameter, and Euler number are calculated. Then, from the analysis of successive sections of extrudates, the pore density has been extrapolated to a 3D value, in number of pores per cubic centimeter. This allowed us to compare our results to literature ones. As for ESEM observations, sample preparation is important since image analysis quality is closely linked to the sample preparation. This is delicate because Eudragit E100 extrudates are very fragile and brittle. For example, if the pore edges are not sharp enough, the detection of pores by threshold search becomes difficult and small pores created by gradient of colors are taken into account that do not correspond to a true porosity. Thus, the pore size distribution obtained by the watershed segmentation may be artificially widened, average diameters underestimated and cell density overestimated.

Finally, we determine the maximum total time required for complete solubilization of CO_2 into the fluid/melt phases and comparing with the residence time inside the extruder previously determined.[14] The total mixing time required for complete homogenization of the CO_2/polymer melts divides in two parts: the distributive mixing time t_m and the diffusion time t_d[21,22] defined by eqs. (2) and (4).

$$t_d = \frac{S^2}{D} \tag{2}$$

$$S = \frac{h_0}{\dot{\gamma}} \tag{3}$$

where D is the diffusivity of the fluid in the melt, $\dot{\gamma}$ the shear rate, x the volume fraction of the minor component, and h_0 is the original striation thickness equal to the channel depth, constant at 0.15 cm.

$$t_m = \frac{h_0}{\dot{\gamma} l_m} \tag{4}$$

with,

$$l_m = \sqrt[3]{\frac{h_0 D}{2\dot{\gamma}}} \tag{5}$$

RESULTS AND DISCUSSION

Torque evolution

Figure 3 shows the torque C evolution versus the CO_2 mass percent in the extruder. Torque first decreases while the CO_2 concentration increases,

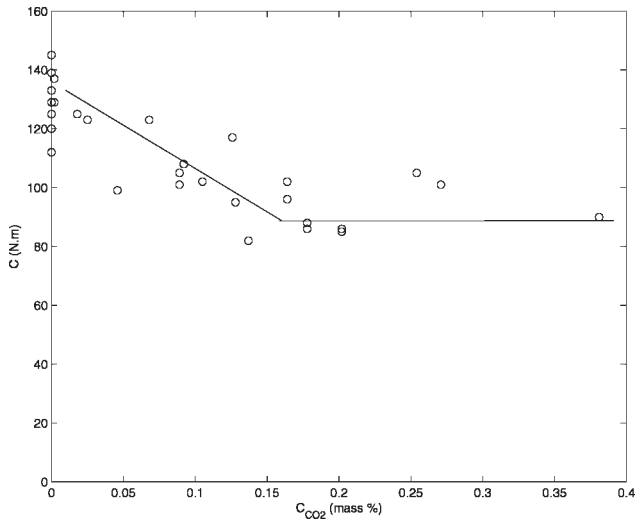

Figure 3 Torque according to the CO_2 concentration.

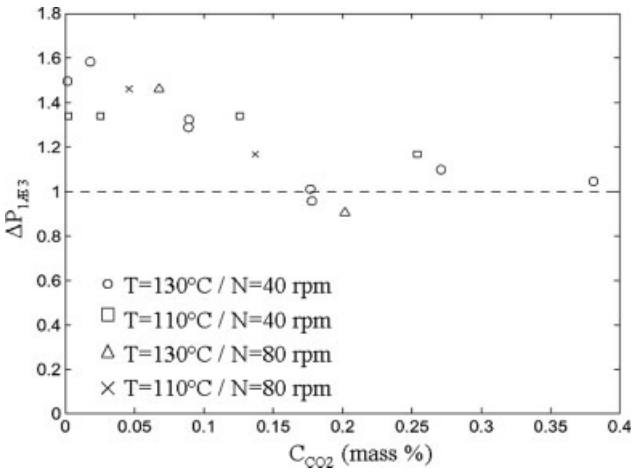

Figure 4 Pressure drop ratio between the entrance of pumping zone and the die according to the CO_2 concentration.

and then, beyond 0.15% of CO_2, it remains roughly constant, equal to 80 N/m.

The torque reflects the required motor power to fix the screw speed and to flow the polymer inside the extruder. The polymer opposes a resistance to its flow because of its viscosity. Thus, the torque reflects the processed material viscosity. Increasing the CO_2 concentration decreases this viscosity and consequently, decreases the torque value. Gourgouillon et al.[7] and Areerat et al.[23] have shown that a dissolved supercritical fluid into a polymer implies the decrease of the melt viscosity.

From 0.15% of CO_2, the viscosity evolves no more. Even though the CO_2 quantity is probably smaller than the saturation concentration in the polymer at the injection conditions, dissolved CO_2 quantity does not increase. We can notice that the pressure evolves between the CO_2 injection part and the die (from 13 to 5.8 MPa; Fig. 4). Consequently, there is a decrease of the CO_2 solubility in the polymer. Moreover, the mixing time ($t_m + t_d$) of CO_2-Eudragit E100 blend must be considered (Table II). Whatever the experiment, the diffusivity of the fluid in the melt, D, is considered as constant at 1.04×10^{-10} m^2/s and the shear rate is calculated by the eq. (6).

$$\dot{\gamma} = \frac{2\pi D_2 N}{60(D_1 - D_2)} \tag{6}$$

TABLE II
Mixing Times, Expansion, Mean Surface Equivalent Diameters, and Cell Density for Different Experiments

No.	t_m (s)	t_d (s)	ε	Diameter eq. (μm)	Pores number (m^{-3})
1	221	110	6.72	161 ± 11	$9.88 \times 10^{13} \pm 3.23 \times 10^{13}$
2	279	139	10.85	About 1200	$<2.57 \times 10^{12}$
3	211	106	6.65	155 ± 11	$1.02 \times 10^{14} \pm 2.99 \times 10^{13}$
4	274	137	9.80	About 1200	$<4.56 \times 10^{11}$
5	106	53	2.99	148 ± 16	$1.13 \times 10^{14} \pm 4.35 \times 10^{13}$
6	133	66	8.20	About 1200	$<4.30 \times 10^{12}$
7	102	51	3.21	154 ± 22	$1.0 \times 10^{14} \pm 3.30 \times 10^{13}$
8	132	66	7.72	–	–
9	141	70	5.91	–	–
10	141	70	5.69	–	–
11	141	70	5.98	About 800	$<7.30 \times 10^{13}$
12	276	138	9.43	–	–
13	102	51	3.26	–	–
14	215	107	6.82	–	–
15	150	75	4.61	–	–
16	176	88	6.33	67 ± 16	$2.57 \times 10^{15} \pm 0.58 \times 10^{15}$
17	816	408	7.28	–	–
18	174	87	2.80	47 ± 8	$1.80 \times 10^{16} \pm 9.43 \times 10^{15}$
19	645	323	3.64	168 ± 12	$2.60 \times 10^{13} \pm 1.40 \times 10^{13}$
20	139	70	3.79	163 ± 13	$7.45 \times 10^{13} \pm 2.95 \times 10^{13}$

where N is the value of screw speed, D_1 and D_2 are diameters of screw and extruder, respectively.

Whatever CO_2 concentrations, the residence time in extruder (i.e., about 200 s) is smaller than the evaluated mixing time and consequently, CO_2-Eudragit E100 blend would not be at thermodynamic equilibrium. Thus, thermodynamic and kinetic phenomena may explain why the torque evolves no more above a CO_2 concentration of 0.15%.

Pressure evolution

To observe only the effect of CO_2 on the pressure, we have calculated a ratio of pressure drop with CO_2 or without CO_2, defined by the eq. (7).

$$\Delta P_{1\to 3} = \frac{(P_1 - P_3)_{\text{with}CO_2}}{(P_1 - P_3)_{\text{without}CO_2}} \tag{7}$$

Figure 4 shows the pressure drop between the CO_2 injection part and the die versus the CO_2 concentration. Like for the torque, pressure drop first decreases while the CO_2 concentration increases, and then, from 0.18–0.2% of CO_2, it remains roughly constant, equal to 1. The decreasing of the pressure drop with the rise in CO_2 concentration reflects the dissolution of CO_2 into the polymer.

We can notice that mainly, the pressure drop with CO_2 is higher than without CO_2. Inside the barrel, near the die, the main flow is governed by the summation of two flows. The first is a shear flow and the second a Poiseuille flow.[24] The shear flow is created by the screw speed and the Poiseuille flow by the pressure through the die. Consequently, the velocity profile $u_Z(\xi)$ evolves with a pressure gradient along the pumping zone, i.e., between P_1 and P_3[25]:

$$u_z(\xi) = v_{\text{Fz}}\xi + \frac{P_1 - P_3}{2\eta Z_p}\xi(\xi - 1) \tag{8}$$

v_{Fz} is the relative speed of the barrel, Z_p the length of the channel, ξ the position of the particle according to the channel height (equal to y/H, y the position on y-axis and H the depth of the channel), η the viscosity of the polymer. For a given temperature and screw speed, the parameters v_{Fz}, Z_p, and ξ are constant. It is possible to express the pressure drop ratio according to the parameters of eq. (9).

$$\frac{[P_1 - P_3]_{\text{with}CO_2}}{[P_1 - P_3]_{\text{without}CO_2}} = \frac{[u_z(\xi) - v_{\text{Fz}}(\xi)]_{\text{with}CO_2}}{[u_z(\xi) - v_{\text{Fz}}(\xi)]_{\text{without}CO_2}} \frac{\eta_{\text{with}CO_2}}{\eta_{\text{without}CO_2}} \tag{9}$$

However, the viscosity of the polymer decreases with the CO_2 concentration. Thus, the ratio of viscosity is lower than 1. The relative velocity of the barrel v_{Fz} remains constant with and without CO_2, thus, the speed ratio will be higher than 1. Consequently, it seems that at low CO_2 concentration, the pressure drop is governed rather by the speed evolution than by the viscosity ratio. When CO_2 concentration increases, the lowering of the viscosity becomes consequent. Finally, there is an equilibrium between the two ratios and we obtain the same pressure drop with and without CO_2 in the process.

Reproducibility

Table II shows the obtained results: the characteristic times (mixing and diffusion), expansion rate ε, the mean surface equivalent diameter of the pores, and the density of the cells.

To check the results reproducibility, an experiment with a die temperature of 120°C, a screw speed of 60 rpm, and a CO_2 volumetric flow rate of 0.1 cm^3/min, has been repeated three times (experiments 9, 10, and 11). Pressure, temperature, and torque within the extruder were the same for each experiment. The expansion rate was 5.84 $\pm$ 0.15. The standard deviation obtained on the expansion rates is roughly the same as the experimental one linked to the apparent and the solid density measurements. We can conclude that the experiments are reproducible.

Effect of screw speed

First, we measured the evolution of expansion rate with the screw speed. The expansion rate remained nearly constant when screw speed increases from 40 to 80 rpm. A 1% increase in porosity was obtained which was not significant and consequently, the screw speed is not an influent operating parameter for the polymer expansion.

Yet, it is difficult to study only the effect of the screw speed. Indeed, an increase of screw speed implies a decrease of CO_2 weight ratio (for a fixed volume flow rate of CO_2). And both have opposite effects on viscosity; a screw speed increase means higher shear rates and lower viscosities and a CO_2 ratio decrease means higher viscosities. However, we can notice that at 110°C and at 130°C (i.e., experiments 1 to 4), the average diameters do not evolve (i.e., 0.158 mm at 110°C and about 1.2 mm at 130°C) whatever the screw speed. This is confirmed by the structure of the samples which is the same (Fig. 5). Thus, we can conclude that the structure of the extrudates does not evolve by increasing the screw speed increase (in the range 40–80 rpm) because of the subsequent CO_2 weight ratio decrease.

Effect of the die temperature

Figure 6 shows that expansion increases with the temperature of the matter T_2, inside the die (the

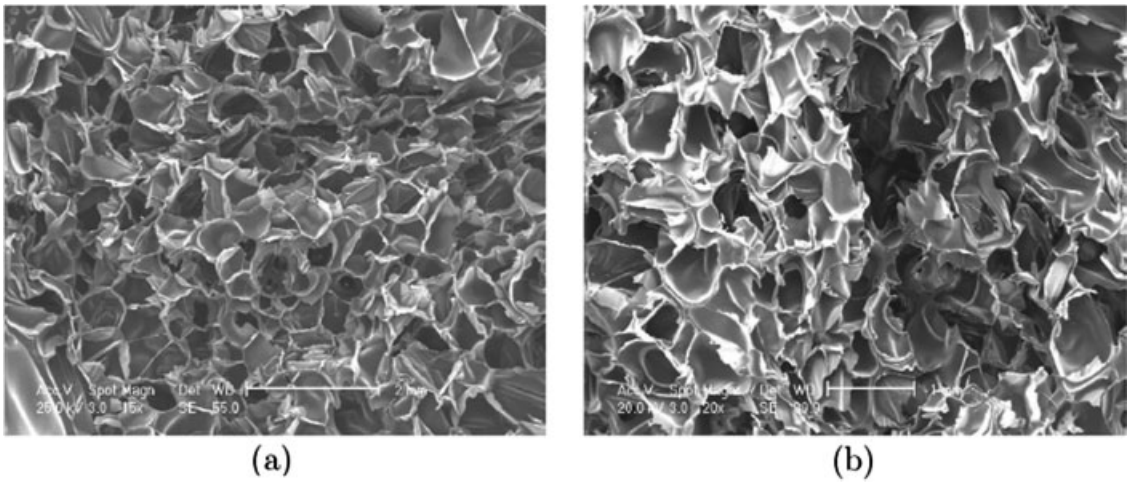

Figure 5 SEM pictures of samples processed at $T = 110°C$, (a) $N = 40$ rpm and 0.126% of CO_2, (b) $N = 80$ rpm and 0.068% of CO_2 (Experiments 1 and 3).

evolution is the same with T_e) whatever the screw speed and the CO_2 concentration. Sauceau et al.[26] found the same results with polystyrene, but Park et al.[27] found that the expansion rate decreases with the increase of polymer temperature. They suggest that the CO_2 diffusion towards outside the extrudate is faster when the polymer surface cools slowly. This implies a high shrinkage at the die outlet. As the polymer is different and the temperatures used are lower than those of Park et al.,[27] the contraction phenomenon is limited in this study. Moreover, a rise in temperature lowers the polymer viscosity, and thus, favors the growth of the bubbles, leading to an increase of the expansion rate.[28] Finally, at 130°C, the time necessary to freeze the structure of the polymer is longer than at 110°C, and consequently, the expansion rates are higher.

Figure 7 shows the evolution of the pore equivalent diameter d_p according to the temperature, for all experiments of Table II. Whatever the screw speed and the CO_2 concentration, the cell size increases with temperature, even for experiments carried out at the lowest CO_2 concentrations, i.e., at 0.002%. Pore equivalent diameter of 47 and 67 μm at 110°C and 130°C, respectively are obtained. This confirms the significant effect of temperature on the growth phenomenon. Figure 8 shows typical pictures taken from two typical samples processed at 130°C and 110°C (above 0.002% of CO_2). The sample picture shows porous heterogeneity. Indeed, there are more pores on the exterior section and they are smaller than those located in the center of the extrudate. The first phenomenon occurring is nucleation, and then growth, which is inhibited on the exterior section by the peripheral water-cooling, leading to smaller pores. We can also notice that the surface of the central cells is not smooth and has some cavities. This may be due to a coalescence phenomenon

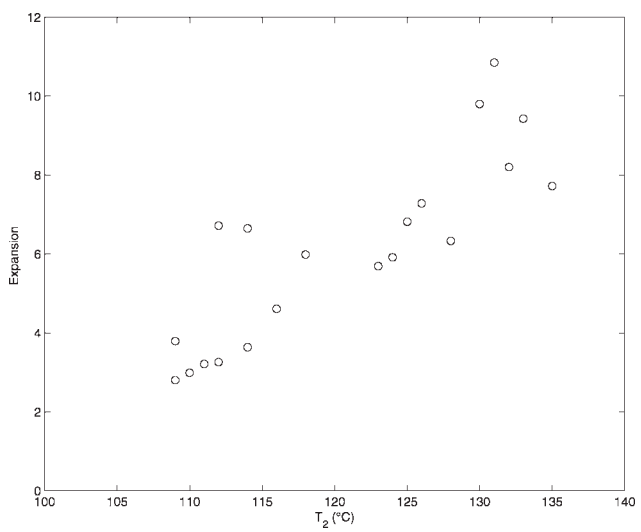

Figure 6 Expansion according to the melt temperature.

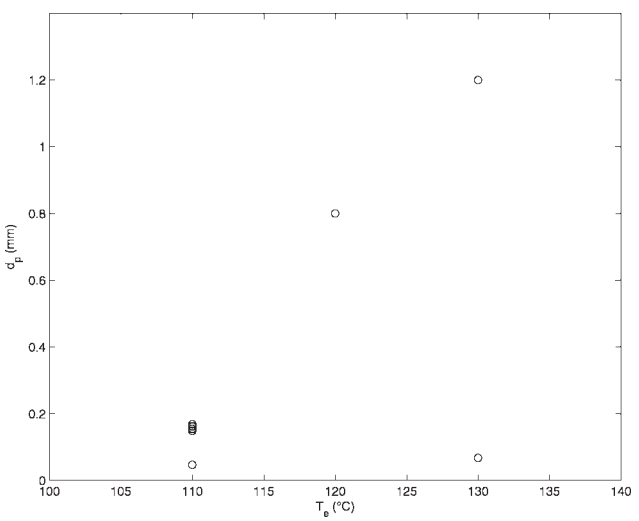

Figure 7 Cell size according to the die temperature.

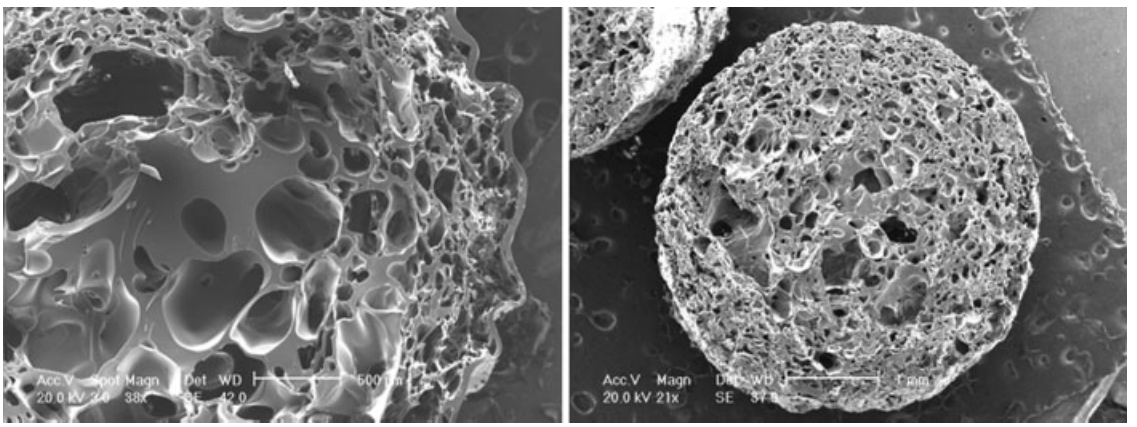

Figure 8 SEM pictures of samples (a) $T = 110°C$ and (b) $T = 130°C$ (experiments 16 and 18).

simultaneous to the growth one. The thick outside wall on picture 8(a) is due to the fast water-cooling. It increases the material viscosity and consequently the retractile force restricting cell growth to increase.[29,30]

Moreover, the cell density according to the die temperature is given in Figure 9. This one appears roughly constant between 110°C and 120°C, then lowers with an increasing temperature up to 130°C. At low CO_2 concentration, the cell density is higher, but follows the same evolution.

Finally, an increase of the temperature favors the pore expansion and the cell size and decreases the cell density. We can conclude that growth and coalescence phenomena are favored when temperature increases and lead to larger porosity.

Effect of CO_2 weight ratio

Figure 10 shows the influence of CO_2 concentration on the expansion rate. For both temperatures, the evolution of the expansion rate is the same. It increases with CO_2 up to 0.1%, and then it decreases. The relationship between CO_2 concentration and expansion rate is complex because many physical properties of Eudragit/CO_2 blends depend on this concentration.

Increasing the CO_2 concentration reduces the interfacial tension and consequently favors the homogeneous nucleation. This leads in turn to a decrease of the Weber number defined as the ratio between surface forces that prevents the break-up and shear forces that are responsible for the break-up of a bubble. Thus, it prevents the coalescence phenomenon.

Increasing the CO_2 concentration diminishes the viscosity of the polymer, and hence, favors growth and coalescence phenomena.[18] Yet, this decrease lowers the residence time of the polymer inside the extruder.[14] These complex influences reflect itself on the structure of the extrudates.

Generally, the porosity obtained was rather a macroporosity with a mean diameter higher than the

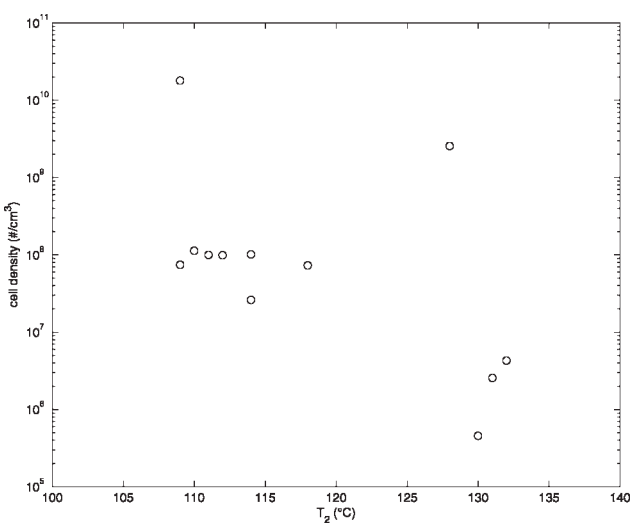

Figure 9 Cell density according to the melt temperature.

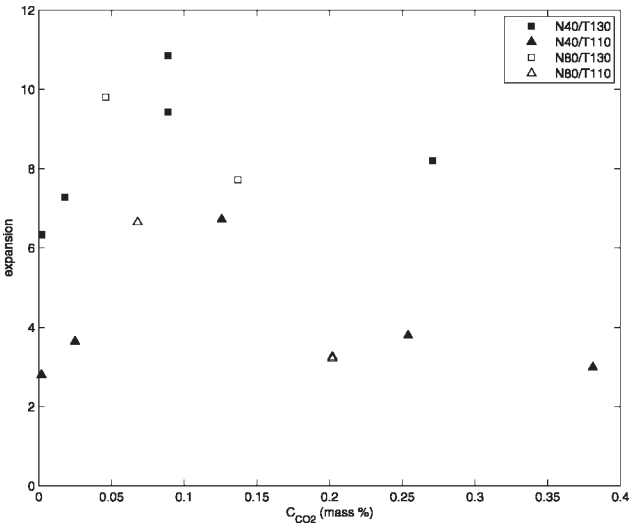

Figure 10 Expansion according to the CO_2 concentration.

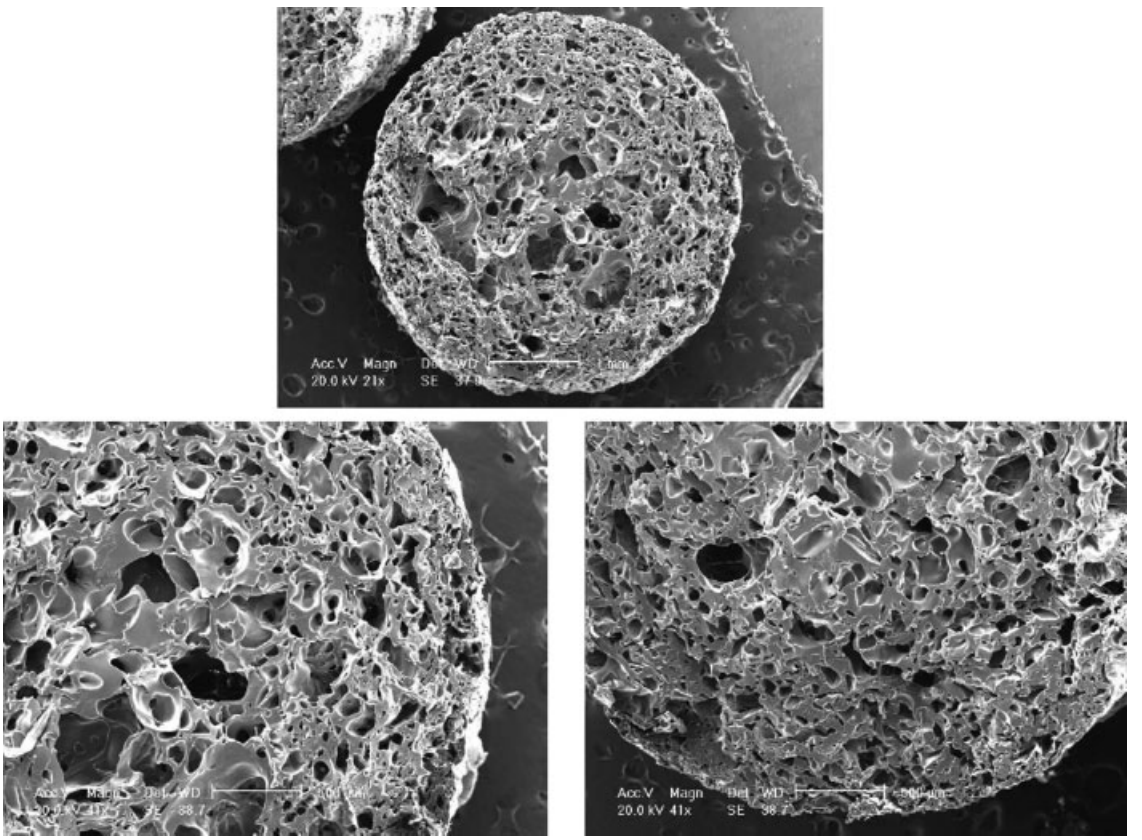

Figure 11 SEM pictures of samples at 110°C, 40 rpm, and 0.002% of CO_2 (experiment 18).

order of magnitude given in the literature for polymers foams, i.e., 10 μm.[31] The cell density is smaller than those given in the literature, i.e., from 10^{15} to 10^{21} pores/m^3,[21] excepted for small CO_2 concentrations. Indeed, for experiments 12 and 18, cell density is similar to those in literature, i.e., 2.10^{15} and 2.10^{16} pores/m^3. At higher CO_2 concentrations (above 0.1 %), the small cell density and the macroporosity may be explained by an outmost predominant growth phenomenon but also probably a heterogeneous polymer-CO_2 blend in the extruder for some CO_2 concentrations where CO_2 could be present in excess. Consequently, this favors nucleation around the existing bubbles and their growth and this enhances the macropores development to the detriment of the small pores.[32]

At low CO_2 concentration, the structure of samples was homogeneous (Fig. 11). Only in the center of the sample, there were larger pores. This is an effect of the peripheral water-cooling and confirms the significant effect of the temperature.

Finally, Table II shows that whatever the temperature, the cell diameter increased with CO_2 up to 0.05% and then remained constant. Moreover, the cell density declines with CO_2 up to 0.05%, then it rose and finally stayed constant (Fig. 12). Consequently, there are three steps in the evolution with the CO_2 concentration. First, expansion and cell size increased while cell density decreased. That means that a small amount of CO_2 favors growth and coalescence phenomena. Second, expansion and cell density went up, but the pores diameter remained constant. Only a nucleation phenomenon can explain an increase in the cell number. The quantity of CO_2 was high enough to modify the physical properties

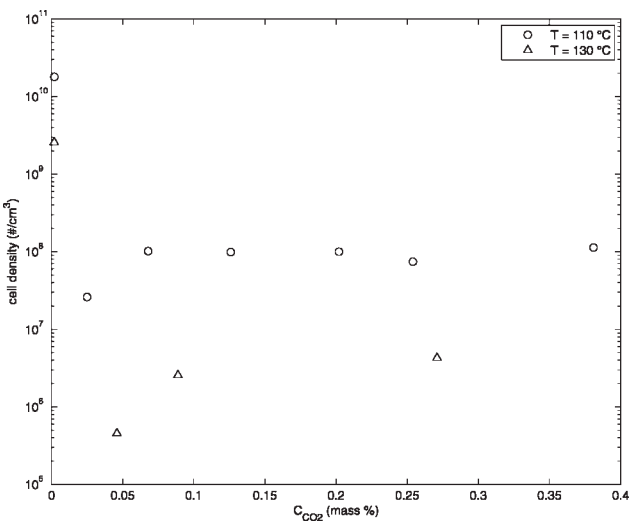

Figure 12 Cell density according to the CO_2 concentration for two temperatures.

of Eudragit/CO_2 melts (interfacial tension and viscosity) and hence, the homogeneous nucleation was favored. Third, the expansion lessened and cell size and density were constant. When the CO_2 concentration was higher than 0.15%, CO_2/Eudragit melt might not be in single-phase. Excess CO_2 may explain the lower expansion by shrinkage of the polymer at the die.

CONCLUSION

A process based on the extrusion in a single-screw extruder coupled with supercritical carbon dioxide ($scCO_2$) was implemented. $ScCO_2$ modifies the rheological properties of the polymeric material in the barrel of the extruder and acts as a blowing agent during the relaxation at the passage through the die. It allows the injection of $scCO_2$ into the melt, the mixing of both components and the creation of porosity into the extruded polymer. In this work, it was applied to Eudragit E100, a biocompatible polymer. The effects of screw speed, die temperature, and CO_2 concentration on material porosity were studied. Eudragit E100 foams with porosity from 65–90% were obtained. Screw speed showed no significant effect on the structure of the material. On the contrary, temperature reveals to be the most significant parameter. A higher temperature enhances the growth phenomenon, consequently, the expansion rate and the average diameter increase. Moreover, coalescence phenomenon is favored by high temperature. The effect of CO_2 concentration is far more complicated because several physical properties of Eudragit/CO_2 blends depend on this concentration. At low concentrations (i.e., around 0.002% weight), much denser microcellular foams were obtained, with smaller pores (around 50–60 μm) and high cell densities (10^{15}–10^{16} cells/m^3). This research is aimed at making matrices for solid dispersions of active molecules. This study shows that it is possible to work at milder operating conditions than usual extrusion process. A temperature of 110°C is not a very hard condition and allows the addition of an active drug in further studies.

References

1. Rauwendaal, C. Polymer Extrusion; Hanser Publishers: München, 2001.
2. Eckert, C.; Knutson, B.; Debenedetti, P. Nature 1996, 383, 313.
3. Kazarian, S. G. Polym Sci 2000, 42, 78.
4. Nalawade, S. P.; Picchioni, F.; Janssen, L. P. B. M. Prog Polym Sci 2006, 31, 19.
5. Aubert, J. H. J Supercrit Fluids 1998, 11, 163.
6. Sato, Y.; Fujiwara, K.; Takikawa, T.; Takishima, S.; Masuoka, H. Fluid Phase Equilib 1999, 162, 276.
7. Gourgouillon, D.; Avelino, H. M. N. T.; Fareleira, J. M. N. A.; Nunes Da Ponte, M. J Supercrit Fluids 1998, 13, 177.
8. Sauceau, M.; Ponomarev, D.; Nikitine, C.; Rodier, E.; Fages, J. Improvement of Extrusion Processes Using Supercritical Carbon Dioxide. Supercritical Fluid and Materials; Vandoeuvre:-France, 2007.
9. Han, J. H.; Han, C. D. J Polym Sci B Polym Phys 1990, 28, 711.
10. Li, H.; Lee, L. J.; Tomasko, D. L. Ind Eng Chem Res 2004, 43, 509.
11. Six, K.; Leuner, C.; Dressman, J.; Verreck, G.; Peeters, J.; Blaton, N.; Augustijns, P.; Kinget, R.; Van Den Mooter, G. J Therm Anal Calorim 2002, 68, 591.
12. Six, K.; Murphy, J.; Weuts, I.; Craig, D. Q. M.; Verreck, G.; Peeters, J.; Brewster, M.; Van Den Mooter, G. Pharm Res 2003, 20, 135.
13. Verreck, G.; Decorte, A.; Tomasko, D.; Arien, A.; Peeters, J.; Rombaut, P.; Van Den Mooter, G.; Brewster, M. E. J Supercrit Fluids 2006, 38, 383.
14. Nikitine, C.; Rodier, E.; Sauceau, M.; Fages, J. Chem Eng Res Des 2009, 87, 809.
15. Dittgen, M.; Durrani, M.; Lehmann, K. S. T. P. Pharma Sci 1997, 7, 403.
16. Rowe, R. C.; Sheskey, P. J.; Owen, S. C. American Pharmaceutical Association and Pharmaceutical Press: London, 2006, 52, p 1.
17. Nikitine, C.; Sauceau, M.; Léonardi, F.; Rodier, E.; Fages, J. 42ème Colloque du Groupe Français de Rhéologie; Clermont-Ferrand: France, 2007.
18. Peng, D.-Y.; Robinson, D. Ind Eng Chem Fundam 1976, 15, 59.
19. Soille, P. Morphological Image Analysis: Principles and Applications; Springer-Verlag: New York, 1999; p 170.
20. Meyer, F. Signal Processing 1994, 38, 113.
21. Kemmere, M. F.; Meyer, T. Supercritical Carbon Dioxide in Polymer Reaction Engineering; Wiley-vch: New York, 2005; Chapter 12.
22. Singh, B.; Rizvi, S. J Food Process Eng 1998, 21, 91.
23. Arrerat, S.; Nagata, T.; Ohshima, M. Polym Eng Sci 2002, 42, 2234.
24. Vergnes, B.; Puissant, S. Techniques de l'ingénieur 2002, p 1.
25. Rauwendaal, C. M. Dekker, Inc.: 1991, Chapter 7, p 365.
26. Sauceau, M.; Nikitine, C.; Rodier, E.; Fages, J. J Supercrit Fluids 2007, 43, 367.
27. Park, C.; Behravesh, C.; Venter, R. Polym Eng Sci 1998, 38, 1812.
28. Han, C. Multiphase Flow in Polymer Processing; Academic Press: New York, 1981.
29. Arora, K. A.; Lesser, A. J.; Mccarthy, T. J. Macromolecules 1998, 31, 4614.
30. Arora, K. A.; Lesser, A. J.; Mccarthy, T. J. Polym Eng Sci 1998, 38, 2055.
31. Fleming, O. S.; Kazarian, S. G.; Kemmere, M. F. Meyer, T., Ed.; Wiley-VCH: Weinheim, 2005; Chapter 10, p 565.
32. Nalawade, S. P.; Nieborg, H. J.; Picchioni, F.; Janssen, L. P. B. M. Powder Technol 2006, 170, 143.